

Disk Substructures at High Angular Resolution Program (DHARP): ?. Multiple ringed-structure in AS209

V. V. GUZMÁN,¹ ET AL1.,² ET AL2.,³ ET AL3.,⁴ AND ET AL4.⁵

¹*Joint ALMA Observatory*

²*Harvard-Smithsonian Center for Astrophysics, 60 Garden Street, Cambridge, MA 02138, USA*

³*Rice University USA*

⁴*Universidad de Chile*

⁵*Others*

ABSTRACT

We present high-angular resolution observations of the 1.2 mm continuum and ^{12}CO 2 – 1 emission from the disk around the T Tauri star AS 209. The dust emission consists of a series of packed rings in the inner ~ 60 au disk, and two bright disks in the outer disk, centered at 74 and 120 au. The gap between the two outer rings is not completely empty, as some faint emission is detected. We also find an additional ring component in the outer disk at 131 au. We modeled the surface brightness emission in the uv-plane and are able reproduce the observations with a simple model of 8 concentric Gaussian rings. Some low level residuals in the inner disk, however, hint at a slightly different inclination for the rings in the inner disk compared to the rings in the outer disk. The ^{12}CO emission also presents substructure. The emission is centrally peaked and extends out to ~ 300 au much farther out than the millimeter dust emission. We find CO emission depletion at three radii in the outer disk, near 75, 120 and 210 au. The outermost gap is located well beyond the edge of the millimeter dust emission, and thus cannot be due to dust opacity and must be caused by a real depletion in the CO abundance due to a chemical effect or by a total gas depletion due to the presence of a planet [Maybe?].

Keywords: circumstellar matter — planetary systems: formation, protoplanetary disks — dust

1. INTRODUCTION

Evolution of disks.

Evidence of radial drift Pérez et al. (2012) and Tazzari et al. (2016). The size of the AS209 disk in the mm continuum varies with wavelength, with the disk being larger at shorter wavelengths (1 / 125 au at 0.88 mm, Perez et al. 2012).

Evidence of dust trapping. Substructure. Rings. What is the origin? Examples of HL Tau, HD163206 and TW Hya, where considerable substructure has been observed.

Case of AS209. Fedele et al. (2018) found 2 rings neat 75 and 130 au. No substructure in the inner disk, however.

Scattered light has also been observed.

Small intro on DHSARP program. In this paper we analyze the dust continuum and ^{12}CO 2 – 1 emission in the disk around the AS 209 star. The $0.9 M_{\odot}$ T Tauri star is a 1.6 Myr old and located 121 ± 1 pc away (REFs).

2. OBSERVATIONS

The observations presented here are part of the DHSARP ALMA Large Program (project code 2016.1.00484.L). The AS 209 disk was observed with ALMA in Band 6 in September 2017 in configurations C40-8/9. Shorter-baselines were observed in May 2017 in configuration

C40-5. We use additional archival data from projects 2013.1.00226 (Huang et al. 2016) and 2015.1.00486.S (Fedele et al. 2018), that provide information on shorter and intermediate baselines, respectively.

A detailed description of the observations and data reduction process can be found in Andrews et al. (2018). Briefly, we first self-calibrated the short baselines, and in a second step self-calibrated the combined observations of short- and long-baselines. The improvement in the signal-to-noise was of a factor of X. The observations were cleaned in CASA 5.1, with multi-scale parameters.. and robust of 0. The resulting image has a beam of $0.04'' \times 0.03''$, position angle of -81° and a rms noise of $1.5 \mu\text{Jy}$.

The solutions of the self-calibration of the continuum emission were then applied to the ^{12}CO data. The molecular line data was first regridded to channels of 0.35 km/s and then cleaned with a robust parameter of 1.0. A Keplerian mask was used to help the cleaning process. We set the deconvolver parameter to *multiscale* in tclean, with scales 0, 10, 25, 75, 150 and 250. The resulting image has a beam of $0.09'' \times 0.07''$, position angle of -83° and a rms noise of 0.77 mJy/beam per channel.

3. RESULTS

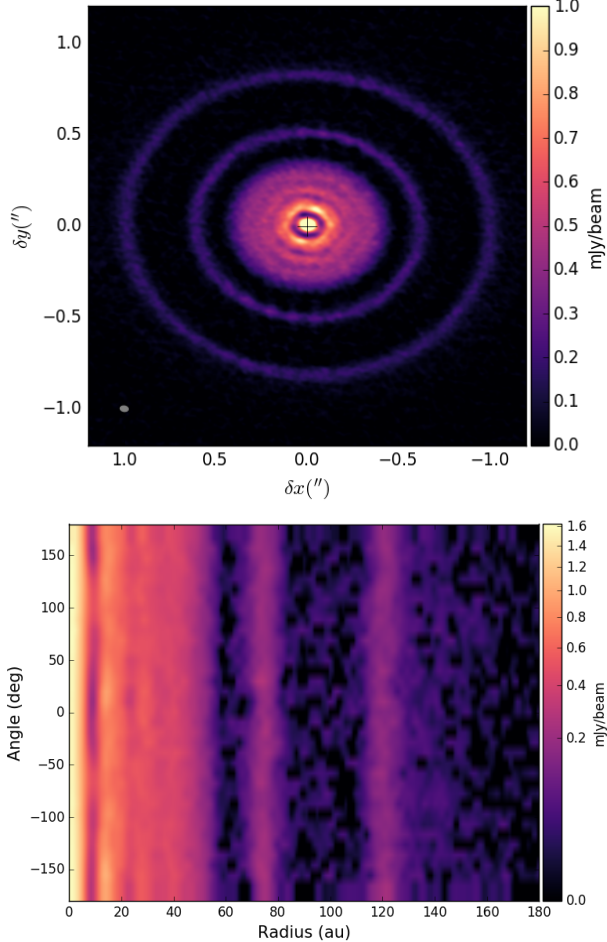


Figure 1. Left: Dust continuum emission map. The beam is shown in the bottom left. Right: Dust continuum emission in polar coordinates.

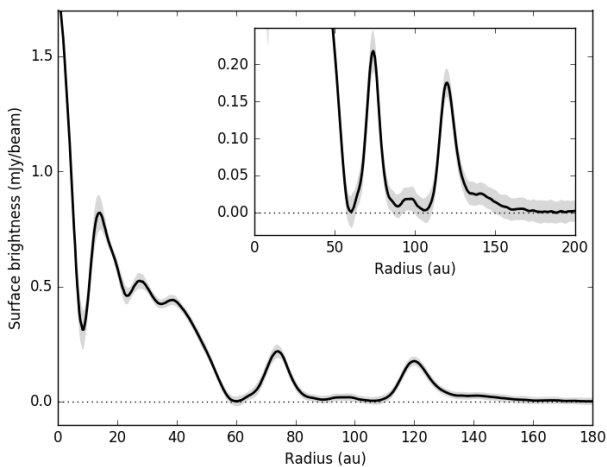


Figure 2. Deprojected radial profiles of the dust continuum emission. The gray ribbon shows the standard deviation at each radius.

In this section we describe the main characteristics of the dust continuum emission from the AS 209 disk, and model the surface brightness in the uv-plane to extract the position and width of the emission components. We then describe the spatial distribution of the ^{12}CO emission and its relation to the dust continuum emission.

3.1. Dust continuum emission

The 1.2 mm dust continuum emission from the AS 209 disk is shown in Fig. 1. The map is shown in the upper panel with the beam size in the bottom left corner. The lower panel shows the emission in polar coordinates, to better visualize the symmetric nature of the emission. The dust emission is characterized by a series of concentric narrow rings and gaps. Fig. 2 shows the deprojected azimuthally averaged emission profile, assuming an inclination of 86° and position angle of 86° for the disk (see section 3.1.1). The emission is centrally peaked and the surface brightness of the rings decreases with radius. A striking characteristic is the difference between the inner < 60 au disk, that consists of several closely packed rings, and the outer > 60 au disk that consists of 2 bright rings that are well separated. The two outer rings have been previously reported by Fedele et al. (2018). The new higher-angular resolution observations reveal the inner disk is not smooth but contains substantial substructure. The rings in the inner disk are blended but resolved. The gap near 100 au is not completely empty of emission, as a bump can be seen in the deprojected radial profile around this radius (better seen in the zoomed panel in Fig. 2). An additional faint component can also be seen at the edge of the disk, just outside the bright ring located at ~ 120 au.

In the next section, we model the emission in the uv-plane to obtain the beam-corrected position and width of the various rings observed in the disk.

3.1.1. Model-fitting in the uv-plane

Given the striking ring-nature of the AS209 disk, we modeled the radial brightness distribution with the sum of concentric Gaussian rings:

$$I(r) = \sum_{i=0}^N A_i \exp(-(r - r_i)^2 / 2\sigma_i^2). \quad (1)$$

The number of rings is chosen by a first eye-examination of the cleaned emission map and the deprojected radial profile (see Figs. 1 and 2). We include 4 rings in the inner (< 60 au) disk and 4 rings in the outer disk. The position of the innermost Gaussian is fixed to zero, i.e., the disk center. Two of outer rings correspond to the faint components near 100 and 140 au. We assume the emission is symmetric, and create synthetic visibilities given by the Henkel transform (Pearson 1999):

$$V(\rho) = 2\pi \int_0^\infty I_\nu(r) J_0(2\pi\rho r) r dr \quad (2)$$

Table 1. Best-fit parameters.

i (deg)	PA (deg)	Offset-x (arcsec)	Offset-y (arcsec)
$34.886_{0.0027}^{0.0015}$	$85.453_{0.0038}^{0.0038}$	$34.886_{0.0027}^{0.0015}$	$34.886_{0.0027}^{0.0015}$
Ring	Rel. Amp	r_i (au)	FWHM (au)
1	$1.000_{0.0065}^{0.0061}$	0.00	$6.64_{0.02}^{0.03}$
2	$0.270_{0.0006}^{0.0007}$	$15.03_{0.01}^{0.02}$	$7.18_{0.04}^{0.04}$
3	$0.133_{0.0005}^{0.0004}$	$26.79_{0.03}^{0.03}$	$11.76_{0.11}^{0.13}$
4	$0.114_{0.0003}^{0.0003}$	$41.38_{0.05}^{0.06}$	$17.35_{0.08}^{0.07}$
5	$0.074_{0.0003}^{0.0003}$	$74.04_{0.01}^{0.01}$	$7.23_{0.04}^{0.03}$
6	$0.004_{0.0001}^{0.0001}$	$90.04_{0.03}^{0.07}$	$19.12_{0.30}^{0.26}$
7	$0.048_{0.0001}^{0.0002}$	$120.42_{0.01}^{0.01}$	$8.26_{0.04}^{0.05}$
8	$0.009_{0.0001}^{0.0000}$	$131.74_{0.13}^{0.13}$	$35.72_{0.17}^{0.17}$

where ρ is the deprojected uv-distance in units of $k\lambda$, r is the radial angular distance from the disk center in units of radians, and J_0 is the zeroth-order Bessel function of the first kind.

The observed visibilities are first deprojected, radially averaged and binned. We include uv-points from 10 to 10000 $k\lambda$, in steps of 10 $k\lambda$. To speed-up the fitting method, we only fit visibilities with uv-distances $< 3000 k\lambda$. The inclination (i), position angle (PA) and center of the disk, given by an offset (δ_x , δ_y), are included as free parameters in the fit. The total number of free parameters is then 27, that is 23 for the Gaussian rings (A_i, r_i, σ_i with i from 1 to 8) and 4 for the disk geometry (i , PA, δ_x, δ_y).

We use the `emcee` package (Foreman-Mackey et al. 2013), which is an implementation of the MCMC method, to sample the posterior distribution and find the best-fit parameters. Table 1 summarizes the best-fit parameters.

We find a disk inclination of 34.9° and a position angle of 85.7° , which are consistent with previous estimates (Fedele et al. 2018). We also find a small offset from the phase center. The four rings in the inner disk are located at 0, 15, 27, 42 au, and have FWHM between 7 and 17 au. The two bright rings in the outer disk are centered at 74 and 120 au. Fedele et al. (2018) found this second ring to be located at 130 au instead of 120 au. The difference is due to the presence of another much fainter ring at 132 au. The faint ring located in between the two bright outer rings is centered at 90 au. The two faint rings in the outer disk are found to be much broader (FWHM of 19 and 36 au) than the bright outer rings. It is possible that a Gaussian representation of these faint emission inside the gaps is not the most accurate.

Fig. 3 shows the observed real part of the deprojected visibilities in black, using the best-fit disk inclination and position angle. The imaginary part of the visibilities are shown in light-blue (shifted by -30 mJy), and remain

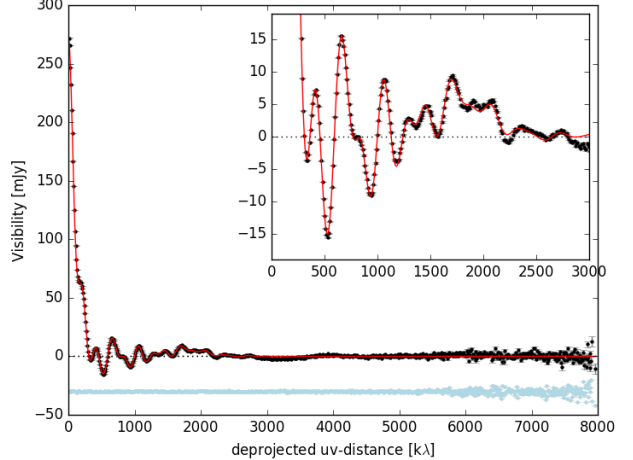


Figure 3. Observed (black) and best-fit model (red) deprojected visibilities. The imaginary part of the observed visibilities are shown in light-blue (shifted to -0.03 Jy). We only fit $u - v$ distances $< 3000 k\lambda$, and assume the emission is axisymmetric.

close to zero for all uv-distance, consistent with symmetric emission of the disk. A zoom of the $< 3000 k\lambda$ visibilities is shown in the upper-right panel of the figure. Our simple parametric model of pure Gaussian rings can recover most of the structure seen in the radially averaged visibility profile. The cleaned image of the best-fit model is shown in Fig. 10. The residuals, corresponding to the cleaned image of residual visibilities ($V_{obs} - V_{model}$) are shown in the right panel of the figure. Our best-fit model successfully reproduces the observations, as seen by the low-level emission in the residuals map. However, an asymmetry is seen in the residuals map near the disk center, which suggests that the rings in the inner ~ 10 au disk have a slightly different inclination than the rest of the disk.

3.2. CO emission

Figure 5 shows the moment-zero map of the CO 2 – 1 line, integrated from -3 to 14 km/s. Pixels with S/N lower than $3 \times \sigma$ have been clipped to highlight the substructure of the emission. The West side of the disk is affected by cloud contamination, which explains the asymmetry of the emission in the disk. The CO emission is 1) centrally peaked, 2) extends much farther out than the millimeter dust emission (out to 300 au), and 3) presents 3 gaps or depletion of emission in the outer disk, near 75, 120 and 210 au. We note this is not an effect of the clipping in the creation the moment-zero map, as the gaps are also seen with even more clarity in the individual channels (see Fig. 6). The gap located near 120 au, spatially coincides with the edge of the millimeter dust emission and the location of the bright outermost dust ring. The innermost gap or CO depletion coincides with

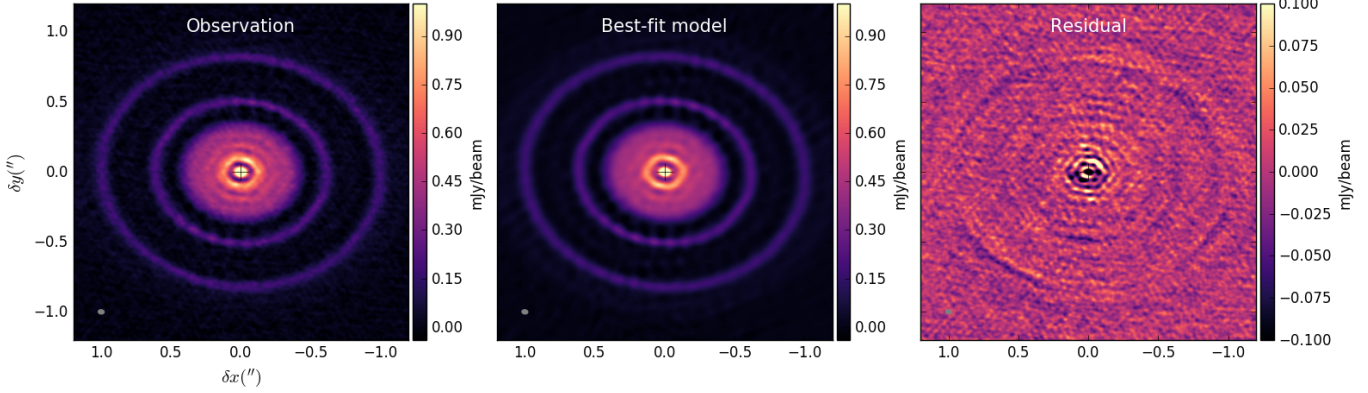


Figure 4. Observed dust emission map (left), the best-fit model (middle) and the residuals (right). **Maybe move to the appendix?**

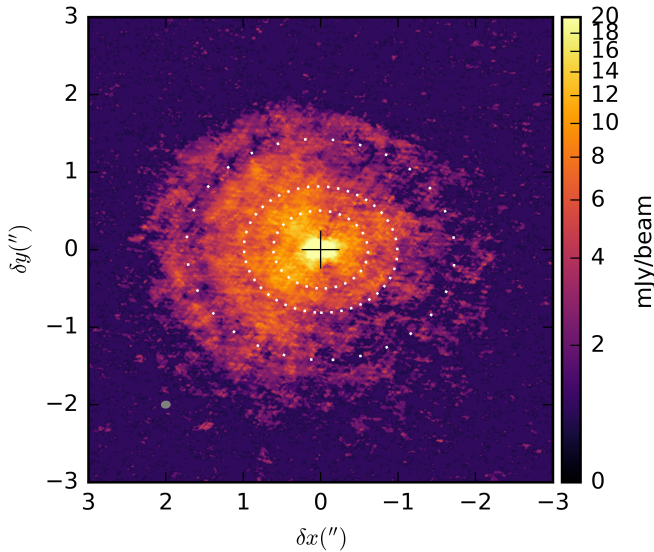


Figure 5. Moment-zero map of the ^{12}CO 2 – 1 line. Emission with signal-to-noise ratio lower than 3 has been clipped. The white dotted lines mark the position of the two brighter outer dust rings, located at 75 and 120 au. The CO gap near 210 au is marked with the largely-spaced dotted white ellipse.

the other outer dust ring near 74 au. This gap is better seen in the channel maps, at a velocity of 5.8 km/s. The spatial coincidence of these two gaps with the location of the millimeter dust rings suggest that the rings are optically thick and are absorbing the CO emission (see the discussion in section 4.2). The third and outermost gap seen in the CO emission is located at 210 au from the central star, well beyond the millimeter dust edge. Therefore, it cannot be explained by dust opacity and must be a real decrease in the abundance of gaseous CO at this radius.

Although some asymmetry along the major axis can be seen in the CO emission, we do not see any major

features pointing to the surface layers of the disk, as can be seen in a very spectacular way towards the disk around the Herbig star HD 163206 (Isella et al. 2018). Given the inclination of the AS 209 disk of 35 degrees, if the disk was flared we should be able to disentangle the lower and upper surface layers in the optically thick CO emission. The fact this is not the case suggest that the gaseous disk, at least the inner part of the disk, is very settled. The case for the outer disk is less clear, due to the lower surface brightness. [Actually, looking more closely at the channel maps, we do see the North part of the disk is brighter, and detect fainter emission from the South side. So, the North part of the disk is closer to us.]

indeed, observations of the scattered light which trace the small grain distribution which should follow that of the gas, show the disk is not very flared (flaring angle of 1.207)

- Dust gaps are not empty. CO emission is present within the gaps.
- CO emission extends outside the millimeter dust edge. This shows the radial drift of large dust grains. Put limit on dust/co emission?
- There are 2 rings outside the millimeter dust emission. Need to confirm this. Maybe we want to show channel maps.
- Note the change of the slope at 50 au.

4. DISCUSSION

4.1. Origin of the dust emission ring-morphology

Using 3D hydrodynamical simulations, Fedele et al. (2018) found that the presence of a giant planet of $\sim 0.8 M_{\text{Saturn}}$ could explain the dust gap seen around 100 au. They also found that the same planet could produce the other prominent gap seen in the continuum at 60 au.

* the properties of the gaps put constraints on the mass of the planet.

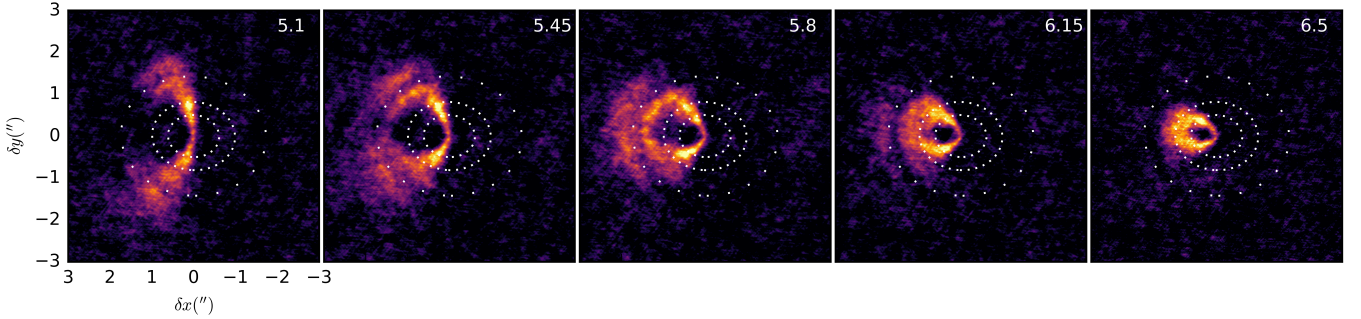


Figure 6. Channel-maps of the ^{12}CO 2 – 1 line emission. Only channels from the uncontaminated East side of the disk are shown. The velocity of each channel is shown in top right corner. The two inner ellipses (dotted lines) mark the position of the two brighter outer dust rings located at 74 and 120 au. A third ellipse (largely-spaced dotted line) corresponding to a projected radius of 210 au is also drawn, to mark the position of a gap of CO emission in the outer disk.

* compare with image of scattered light from [Avenhaus et al. \(2018\)](#). No visible substructure is seen in the scattered light image. Scattered light emission, although faint, is detected up to 200 au. The emission for the AS 209 disk was found to be faint, compact and feature-less in comparison to other disks, despite being one of the most massive disks in the sample. [Avenhaus et al. \(2018\)](#) suggest that this is due to a self-shadowing effect. This means that the small grains have settled substantially towards the midplane (?).

* discuss in the context of the results of Fedele's paper.

* are there any resonances between the rings and/or gaps?

* possible origins: chemistry, GI, planets?

* this is a young system, which means that planet formation starts occurs very early ($\lesssim 1$ Myr) in the evolution of disks.

* compare with other disks? HL Tau, HD 163296, and TW Hya? others from the LP?

4.2. Origin of the CO emission rings and gaps

* two inner gaps/depletion - ζ dust opacity (see [jane's paper](#) and [laura2012](#) and [tazzari2016](#)) normally co emission decreases monotonically, and dust opacity has been found to be negligible due to the low surface dust brightness temperature found in disks (6-10K), which are too low to produce absorption of the lines. However, AS209 has all of the emission in the outer dusty disk concentrated in two narrow rings. However, their peak brightens temperatures of $\sim 0.15 - 0.20$ mJy, corresponding to $\sim 3 - 4$ K, only produce an opacity of $\sim 0.4 - 0.5$ assuming a dust temperature of $\sim 12 - 15$ K (see [Dullemond et al. 2018](#)).

* emission outside dust edge - ζ thermal desorption that brings back CO into the gas-phase

* gap in the outer disk - ζ chemical effect? (see DCO^+ double ring paper) or planet

Most observations of ^{12}CO so far show monotonically decreasing profiles as a function of radius (REFs examples).

[Huang et al. \(2016\)](#) presented CO isotopologue observations of the AS 209 disk at lower angular resolution ($0.6''$), and found that the C^{18}O emission consists of a central peak and a ring component centered at a radius of ~ 150 au. Their optically thick ^{12}CO emission, however, was found to be centrally peaked. The higher angular resolution ^{12}CO observations present some new interesting substructure. In particular, we detect a fainter outer ring centered at ~ 240 au, which was not detected in the C^{18}O emission probably due to the low signal-to-noise. The CO emission thus presents at least 2 ring components located well-beyond the millimeter dust edge and also well outside the expected location of the CO snowline (between 30 and 90 au; ?). The presence of these two rings thus cannot be explained by dust opacity, and suggest that the CO abundance is enhanced at these radii in the outer disk.

A double-ring structure has also been observed before in the IM Lup disk with observations of DCO^+ (?). In that case, the emission can be explained if CO is depleted

The outer ring could be explained by non-thermal desorption in the outer disk due to the lower density, which bring back CO into the gas-phase.

The fact that we can see a gap at ~ 210 au, despite ^{12}CO being optically thick, suggest the depletion is caused by a real decrease in the gas density at this radius at all heights (not only the midplane).

Another possibility to explain the outermost gap seen in the CO emission is by a depletion of H_2 at this radii. This could hint at the presence of a planet located at 210 au that has carved a gap in the disk. Such a planet would be located far outside the current millimeter edge.

* discuss the new [Pinte](#) and [Teague](#) papers, where planets are inferred from deviations of the Keplerian velocities for CO.

- Compare with rings in HL Tau and TWHya. The continuum emission in the AS209 disk shows deeper gaps.

- Discuss possible explanations for the formation of the gaps. Dust trapping (refer to Dullemond et al. 2018). The low viscosity model shown in Fedele’s paper predict that a single planet can create multiple gaps in the disk, but this gaps are not completely empty. We do observe faint emission be-

tween the 2 main outer rings, which is consistent with these models.

- Compare ^{12}CO and dust. Huang et al (2016) detected C^{18}O extended emission that spatially coincides with the outer dust ring. With ^{12}CO we trace the disk surface.

5. SUMMARY

REFERENCES

- Andrews, S. M., Wilner, D. J., Hughes, A. M., Qi, C., & Dullemond, C. P. 2009, ApJ, 700, 1502
- Avenhaus, H., Quanz, S. P., Garufi, A., et al. 2018, arXiv:1803.10882
- Fedele, D., Tazzari, M., Booth, R., et al. 2018, A&A, 610, A24
- Foreman-Mackey, D., Conley, A., Meierjurgen Farr, W., et al. 2013, Astrophysics Source Code Library, ascl:1303.002
- Huang, J., Öberg, K. I., & Andrews, S. M. 2016, ApJL, 823, L18
- Pearson, T. J. 1999, Synthesis Imaging in Radio Astronomy II, 180, 335
- Pérez, L. M., Carpenter, J. M., Chandler, C. J., et al. 2012, ApJL, 760, L17
- Tazzari, M., Testi, L., Ercolano, B., et al. 2016, A&A, 588, A53

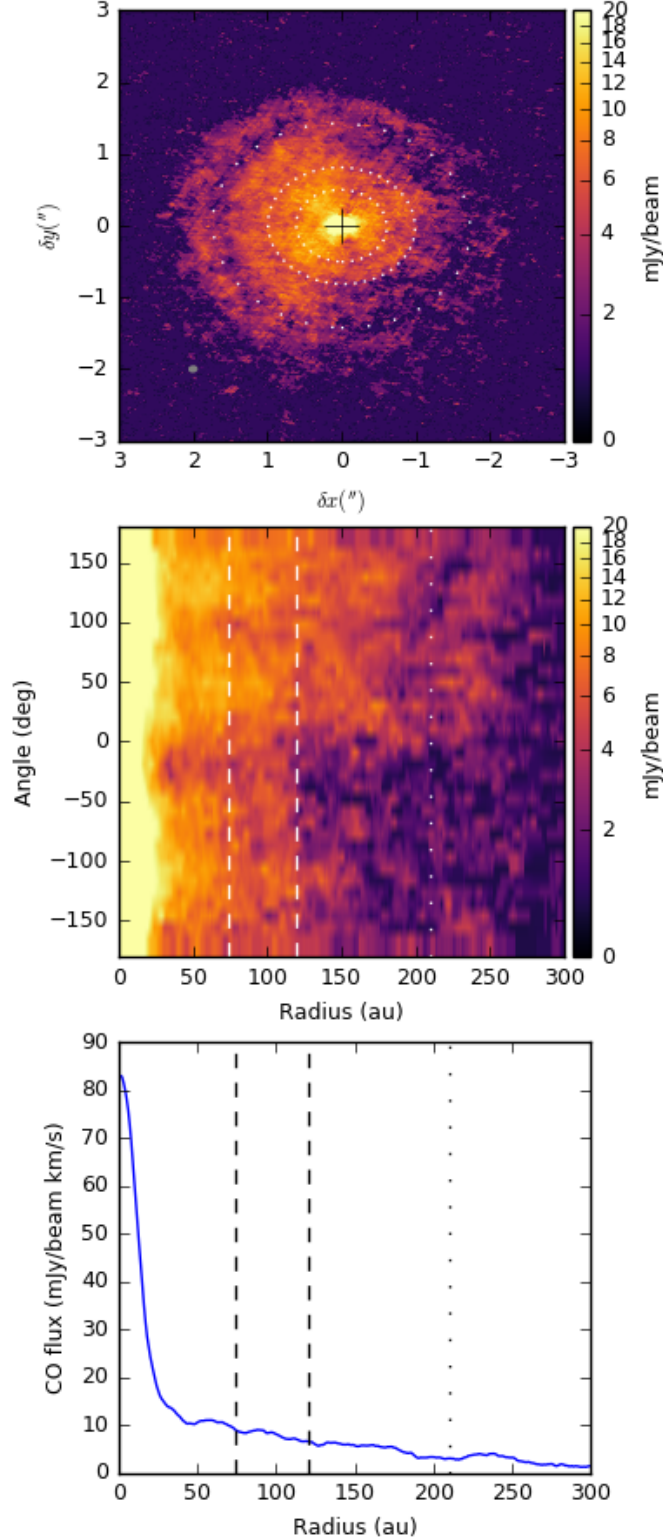


Figure 7. Top: Moment-zero map of the ^{12}CO $2 - 1$ line emission. The white dotted lines mark the position of the two brighter outer dust rings. Middle: CO map shown in polar coordinates. Bottom: Deprojected radial profile of the CO emission. Only the East side of the disk (angles from 0 to 150 degrees) is considered to obtain the radial profile.

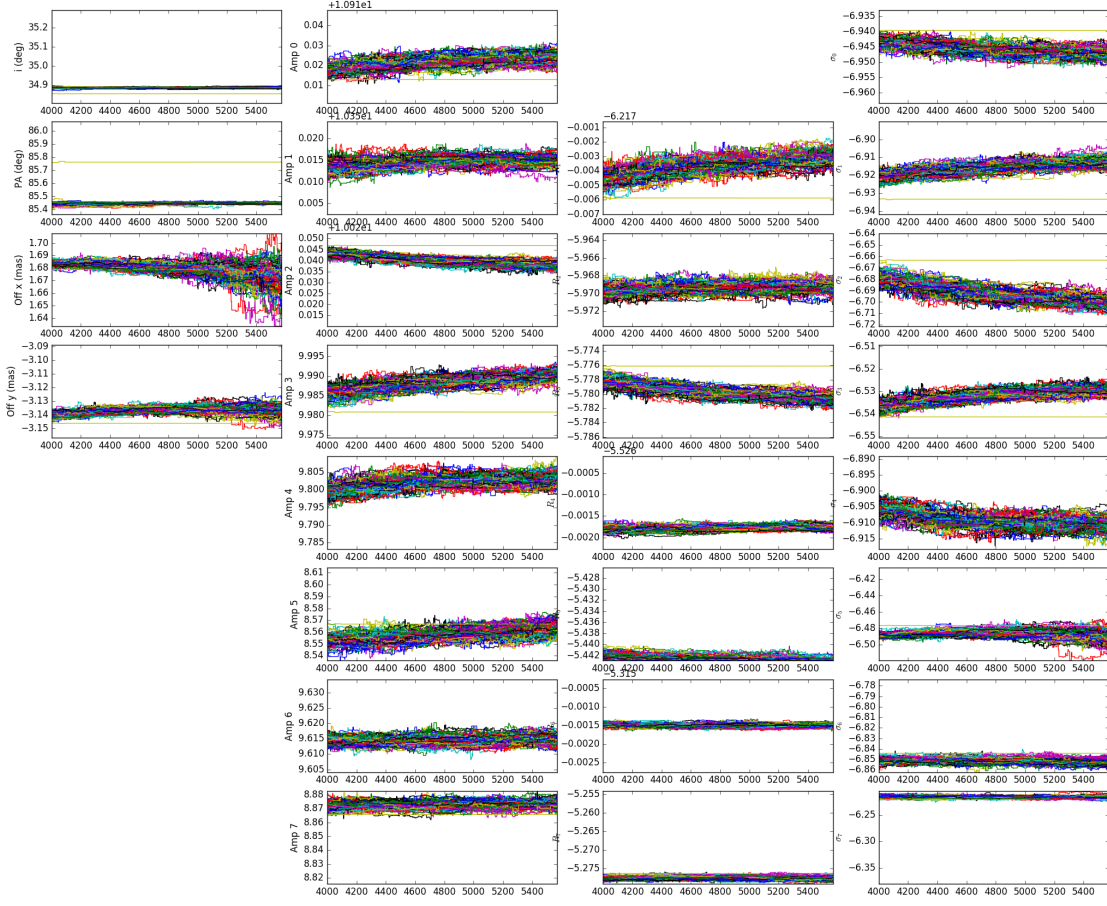


Figure 8. Observed dust emission map (left), the best-fit model (middle) and the residuals (right).

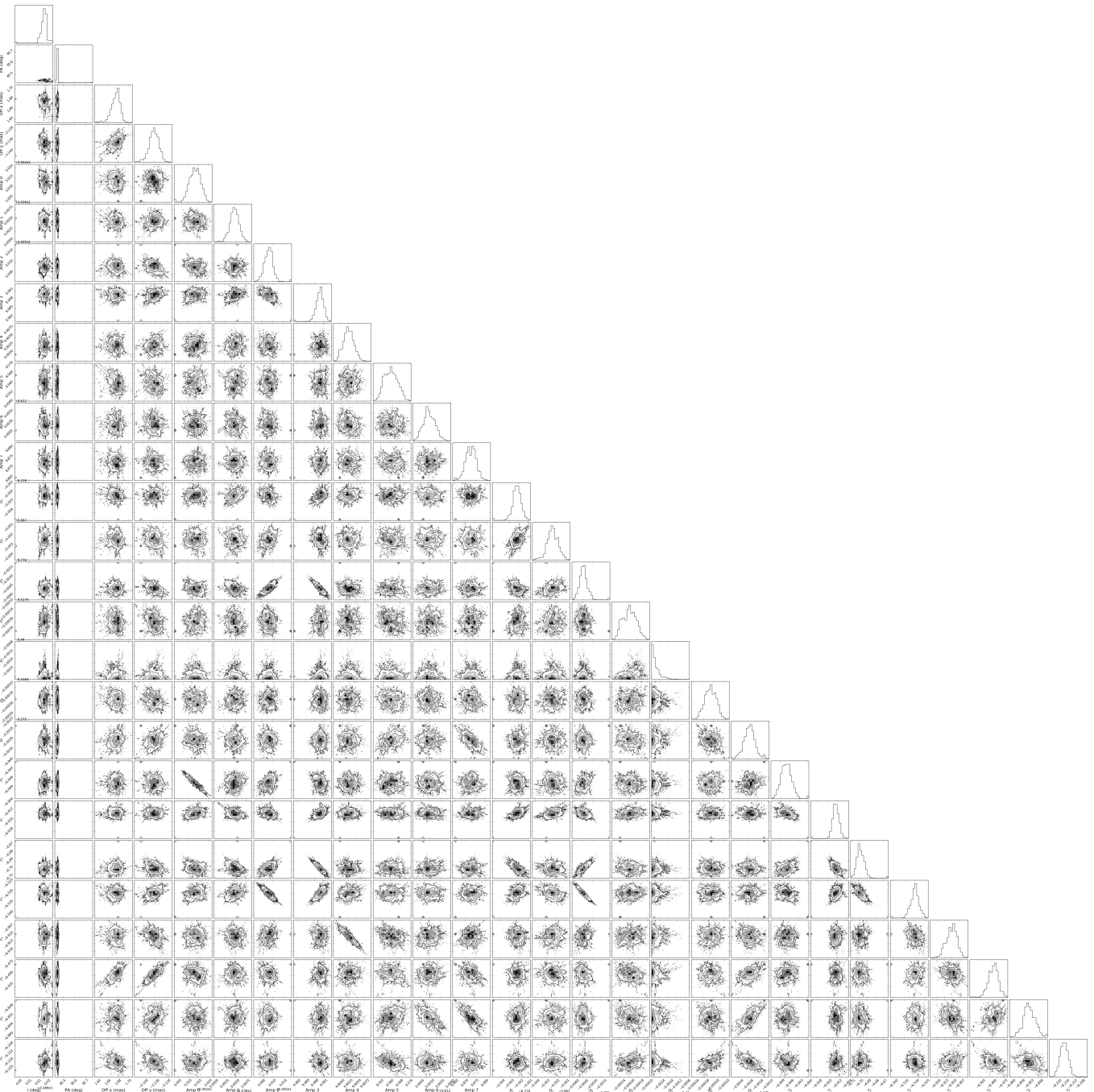


Figure 9. Observed dust emission map (left), the best-fit model (middle) and the residuals (right).